Bipolar Spectral Associative Memories

Ronald G. Spencer, *Member, IEEE*

***Abstract*—Nonlinear spectral associative memories are proposed as quantized frequency domain formulations of nonlinear, recurrent associative memories in which volatile network attractors are instantiated by *attractor waves*. In contrast to conventional associative memories, attractors encoded in the frequency domain by convolution may be viewed as *volatile on-line inputs*, rather than *nonvolatile, off-line parameters*. Spectral memories hold several advantages over conventional associative memories, including *decoder/attractor separability* and *linear scalability*, which make them especially well suited for digital communications. Bit patterns may be transmitted over a noisy channel in a spectral attractor and recovered at the receiver by recurrent, spectral decoding. Massive nonlocal connectivity is realized *virtually*, maintaining high symbol-to-bit ratios while scaling *linearly* with pattern dimension. For n-bit patterns, autoassociative memories achieve the highest noise immunity, whereas heteroassociative memories offer the added flexibility of achieving various code rates, or degrees of extrinsic redundancy. Due to linear scalability, high noise immunity and use of conventional building blocks, spectral associative memories hold much promise for achieving robust communication systems. Simulations are provided showing bit error rates (BERs) for various degrees of decoding time, computational oversampling, and signal-to-noise ratio (SNR).**

***Index Terms*—Associative memory, associative modulation, attractor waves, digital communications, extrinsic redundancy, noise immunity, virtual nonlocal neural connectivity.**

I. Introduction

A. Introduction

SINCE Hopfield's seminal papers in 1982 [1], recurrent associative memories have been studied extensively [2]–[6] and new networks proposed [7]–[9] in which nonlinear feedback is used to recover stored patterns in the presence of noise. Because memory recall is initiated by partial or noisy patterns and is completed without an address, these networks are categorized as content addressable memories (CAMs). A number of CAMs have been implemented in both electronic [10]–[14] and optical [15], [16] forms.

Associative memories bear some resemblance to holograms [17]–[21] due to *extrinsic redundancy* of stored patterns in the matrices that specify neural connectivity. Every neuron's local synaptic weight vector contains information about the global pattern. Like a hologram, the parts make up the whole and the whole makes up the parts; i.e., contained within the pieces of a broken hologram is the image itself. Such high degrees of redundancy lead to noise immunity, but usually at the expense of spatial dimension. Unlike cellular neural networks (CNNs) [22]–[24], which require only local connectivity, CAMs require nonlocal connectivity and therefore scale quadratically or polynomially with pattern dimension.

In this paper, a new kind of network called spectral associative memory (SAM) [25], [26] is proposed. Compared to the conventional formulations, the most distinguishing feature lies in the representation of the attractors. Whereas the attractors of spatial CAMs are embedded into a neural network as an array of synaptic weights, the attractors of spectral CAMs persist transiently as a superposition of waves. Exploiting the orthogonal property of sine and cosine waves and the richness of spectral convolution, nonlocal connectivity may be achieved *virtually*, reducing the spatial dimensions of the hardware and allowing for useful applications in the field of communications. Unlike Hopfield networks, which scale quadratically with pattern dimension, SAMs scale linearly.

The fact that convolution may be used to form associations has been appreciated for several decades in the optical storage field [15]–[21]; however, the main thrust behind such work has been in *nonvolatile* memories where attractors were stored to some medium. The attractors described in this paper are not stored in a neural decoder or glass plate—they are only *expanded* by a neural decoder. Rather than embedding neural attractors, or "memories," directly into the spatial architecture of a network, (Fig. 1) attractors may be created in the frequency domain and transmitted to a spectral neural decoder for recall (Fig. 2). Whereas spatial attractors are inseparable from the neural network in which they are embedded, spectral attractors may exist separately. Upon activation, *temporary basins of attraction* are created in the network's virtual recall potential that cause the neural decoder to unfold one of the memories; a classical analog of Sarfatti–Bohm wave/particle interaction theory in which a pilot wave guides the material state of subneuronal matter into a basin of attraction of the Q landscape [27]. More than one memory pattern may be enfolded and superimposed into the attractor wave at a time, in which case the initial conditions are important, but for simple communication applications only one spectral attractor is allowed to activate the neural decoder at a time for spurious-free recall.

Spectral attractors created from bit patterns may be superimposed into the same attractor wave, radiated into the electromagnetic spectrum, and expanded by a remote decoder with no physical connection. Such a decoder is an *uninstantiated, attractorless decoder* with no net motive until activated by a coherent spectral attractor. Autoassociative spectral decoding is defined as

$$v_i = \operatorname{sgn}\left(\int W(t) v(t) \cos(\omega_{ai} t)\, dt \right); \qquad i = 0, 1, \ldots n-1 \tag{1}$$

Manuscript received May 2, 2000; revised December 4, 2000.

The author is with the Department of Electrical Engineering, Analog and Mixed-Signal Center, Texas A&M University, College Station, TX, 77843–3128 USA (e-mail: rspencer@tamu.edu).

Publisher Item Identifier S 1045-9227(01)03568-8.

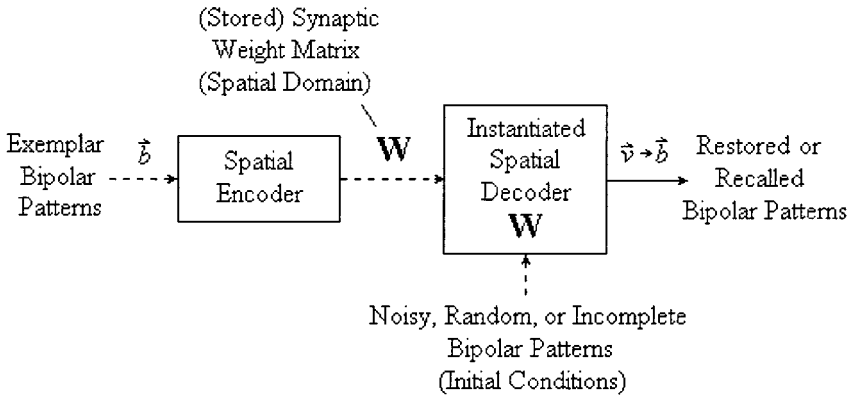

Fig. 1. Schematic of a conventional Hopfield network. Patterns are encoded into a synaptic weight matrix that is *stored* in a neural decoder.

where

- $W(t)$ *attractor wave* which carries at least one enfolded pattern;
- ω_{ai} ith analysis frequency;
- $v(t)$ continuously updated state wave;

$$v(t) = \sum_{i=0}^{n-1} v_i \cos(\omega_{vi} t) \tag{2}$$

where v_i is the ith neural state or recalled bit, ω_{vi} is the ith synthesis frequency defined according to antialiasing constraints. The autoassociative attractor wave is defined as

$$W(t) = k_w \sum_{m=1}^{p} \left(M^{(m)}(t) - I(t) \right) \tag{3}$$

where

- k_w attractor wave scaling factor;
- m pattern index;
- $I(t)$ identity or reference wave for canceling diagonal frequencies;
- $M^{(m)}(t)$ *memory wave* in which a single pattern is enfolded.

Heteroassociative spectral coding does not need reference wave subtraction and requires an additional virtual layer state band and antialiasing constraint.

Conventional associative memories are reviewed in Section II, followed by autoassociative spectral memories in Section III. In-phase (I) and quadrature (I/Q) formulations are presented, followed by antialiasing constraints and scaling complexity. These formulations are distinguished by the attractor wave; in-phase (nonquadrature) coding generates a double-sideband (DSB) attractor, and quadrature coding generates a single-sideband (SSB) attractor. A two-pattern 8×8 example is given to illustrate content addressability. The band structures and antialiasing constraints for heteroassociative spectral memories are presented in Section IV. In Section V, a single-pattern, five-bit autoassociative SAM is characterized in terms of bit error rate (BER) for various decoding times, computational oversampling, and signal-to-noise ratios (SNRs). Conclusions are given in Section VI.

II. Spatial Associative Memories

A. Autoassociative Memories

The conventional Hopfield network [1], is a nonlinear, autoassociative recurrent network in which noiseless patterns are restored from noisy initial conditions (Fig. 1). Noiseless exemplars are stored in a weight matrix that specifies the *spatial connectivity* of the network; a superposition of p synaptic weight matrices formed from p n-dimensional bipolar bit patterns as follows:

$$\mathbf{W} = \frac{1}{p} \sum_{m=1}^{p} \left(\mathbf{M}^{(m)} - \mathbf{I} \right) \tag{4}$$

where $\mathbf{I}$ is the identity matrix and $\mathbf{M}$ is the *memory matrix* formed by the outer product

$$\mathbf{M}^{(m)} = \mathbf{b}^{(m)} \mathbf{b}^{(m)^T} \tag{5}$$

and $\mathbf{b}^{(m)}$ are bit patterns to be stored, where $b_i^{(m)} \in \{-1, +1\}$ and $m = 1, 2, \ldots, p$. Subtracting $\mathbf{I}$ from $\mathbf{M}$ eliminates self-connectivity in the decoder by cancelling the diagonal elements of $\mathbf{W}$.[1]

$\mathbf{W}$ is *stored* in a neural decoder where it persists as a *nonvolatile memory* in the synaptic weights of the network. Because the decoder stores $\mathbf{W}$, the encoder is not needed during recall, denoted by the dashed line in Fig. 1. Noisy patterns are provided as initial conditions, and the neural decoder converges to the closest stored pattern. During recall, n linear combinations of $\mathbf{W}$ and $\mathbf{v}$ are computed, followed by quantization:

$$v_i^{l+1} = \operatorname{sgn}\left(a_i^l\right); \qquad \mathbf{a}^l = \mathbf{W}\mathbf{v}^l \tag{6}$$

where l is the iteration index and update is asynchronous.[2]

B. Heteroassociative Memories

Patterns *pairs* are stored in heteroassociative networks

$$\left\{ \left(\mathbf{b}_1^{(1)}, \mathbf{b}_2^{(1)} \right), \left(\mathbf{b}_1^{(2)}, \mathbf{b}_2^{(2)} \right), \ldots, \left(\mathbf{b}_1^{(p)}, \mathbf{b}_2^{(p)} \right) \right\} \tag{7}$$

[1]Canceling the diagonals is necessary for low-dimensional patterns, but may be neglected for large n.

[2]Asynchronous update is required to avoid limit cycles in the conventional formulation.

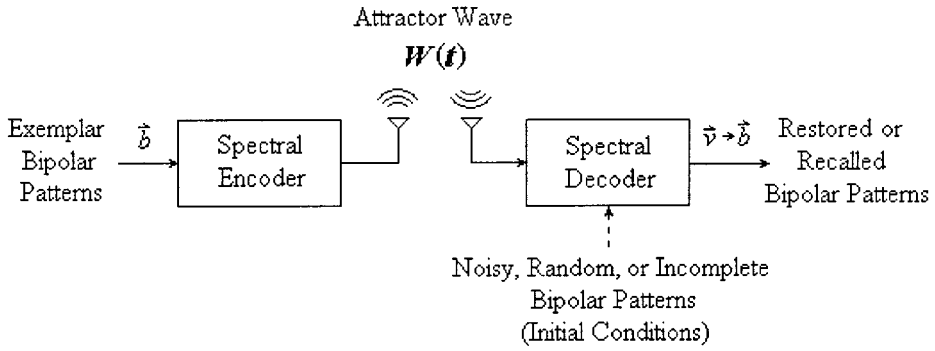

Fig. 2. Schematic of a spectral associative memory. Patterns are encoded into an *attractor wave* that activates a spectral decoder to recall a memory only when the spectral attractor is being transmitted.

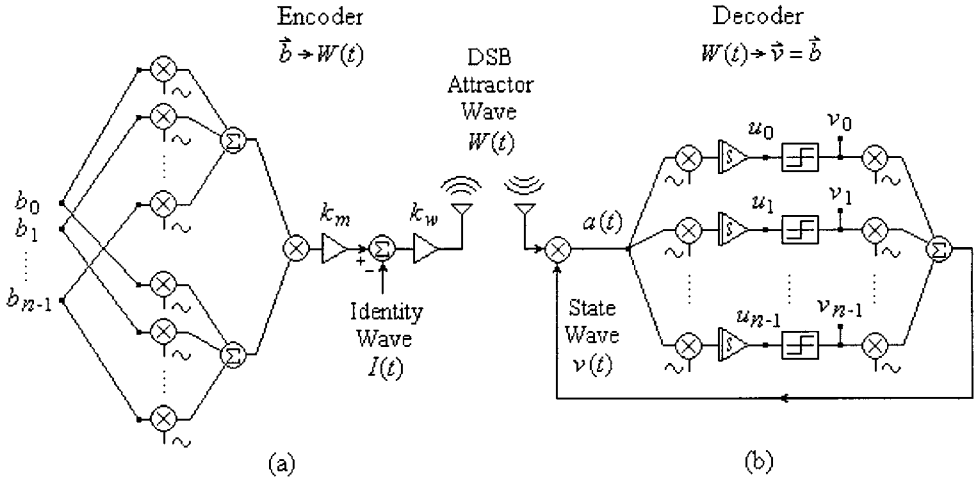

Fig. 3. Block diagram of an autoassociative spectral associative memory with: (a) in-phase encoder and (b) in-phase decoder. Patterns are encoded into the *attractor wave* by associative modulation. The attractor wave creates a temporary basin of attraction in the spectral decoder, which recalls the memory by recurrent associative demodulation. Nonlocal neural connectivity is made *virtually* in the frequency domain.

where $\mathbf{b}_1$ and $\mathbf{b}_2$ are n_1- and n_2-dimensional bipolar patterns, respectively, and p is the number of pairs to be superimposed into the same weight matrix. Heteroassociative or *bidirectional associative memories* (BAMs) [7], [8] have two neural layers, but can be shown to be special cases of the Hopfield network when the two patterns are made into one. The synaptic weight matrix is

$$\mathbf{W} = \frac{1}{p}\sum_{m=1}^{p} \mathbf{b}_1^{(m)}\mathbf{b}_2^{(m)^T} \tag{8}$$

which contains $n_1 n_2$ weights and requires no diagonal cancellation. Heteroassociative recall proceeds in the same manner as autoassociative recall where the state updates are driven by $\mathbf{a}_1 = \mathbf{W}\mathbf{v}_2$ and $\mathbf{a}_2 = \mathbf{W}^T\mathbf{v}_1$. Although the amount of extrinsic redundancy is less than autoassociative redundancy, the hardware still scales polynomially and connectivity is still nonlocal in a two-dimensional (2-D) plane.

III. Autoassociative Spectral Memories

Conventional associative memories may be reformulated in the frequency domain by associative modulation and demodulation. Bit patterns may be encoded into an *attractor wave* that is transmitted to a spectral neural decoder and recalled by spectral convolution, achieving nonlocal neural connectivity virtually with no direct physical connection. See Figs. 2 and 3. Frequency-domain representations, also used in [28], are promising from a very large scale integration (VLSI) standpoint because data that would otherwise be distributed spatially, thus taking up silicon area, may be redistributed in the frequency domain to reduce spatial complexity. Whereas the attractors of conventional decoders are embedded directly into the neural decoder, spectral attractors may exist separately from the neural decoder. As such, the neural decoder recalls nothing until an attractor wave activates it. Furthermore, the memory is recalled only as long as the attractor wave is sustained—a volatile memory.

A. Spectral Encoding

A number of n-dimensional bipolar bit patterns formed by spectral convolution may be superimposed into one composite attractor wave as follows:

$$W(t) = k_w \sum_{m=1}^{p} \left(M^{(m)}(t) - I(t) \right) \tag{9}$$

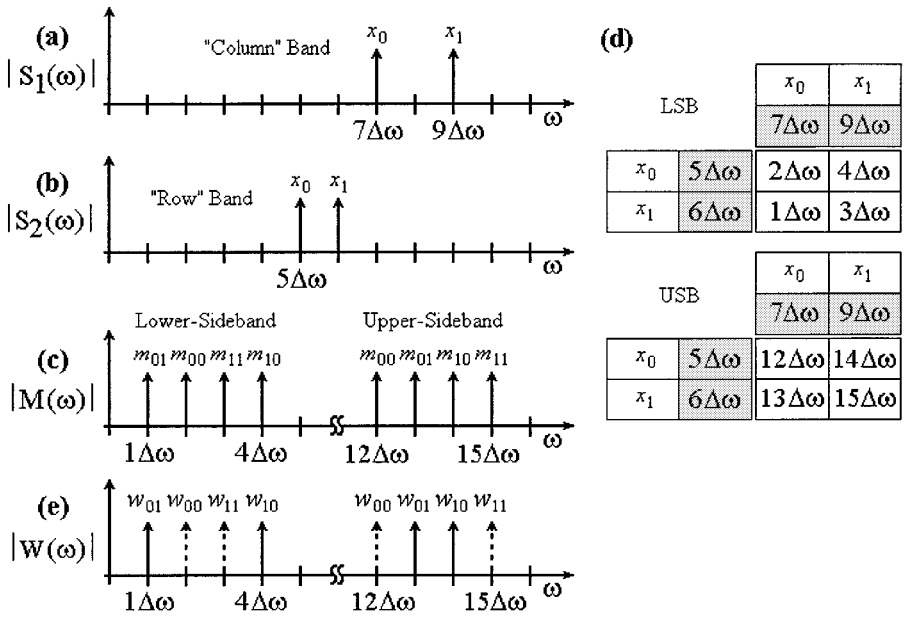

Fig. 4. Example of 2-D associative modulation.

where

k_w attractor wave scaling factor;

m pattern index;

$I(t)$ identity or reference wave for canceling virtual self-connectivity;

$M(t)$ memory wave in which the bit patterns are encoded.

See Fig. 3(a). The DSB version of the memory wave is formed by *in-phase coding*, or associative modulation as follows:

$$M_{\mathrm{DSB}}^{(m)}(t) = k_m s_{I1}^{(m)}(t) s_{I2}^{(m)}(t); \qquad k_m = 2\sqrt{n} \tag{10}$$

where $s_{I1(2)}(t)$ carry the encoded patterns as follows:

$$s_{I1(2)}^{(m)}(t) = k_{s1(2)} \sum_{i=0}^{n-1} b_i^{(m)} \cos\left(\omega_{S1(2)_i} t\right); \qquad k_{s1(2)} = \frac{1}{\sqrt{n}} \tag{11}$$

and $b_i^{(m)} \in \{-1, +1\}$. The two nonoverlapping band structures used for autoassociative in-phase coding are given by

$$\omega_{S1_i} = \omega_{S1.L} + in\Delta\omega, \qquad \omega_{S2_i} = \omega_{S2.L} + i\Delta\omega \tag{12}$$

where $i = 0, 1, \ldots n-1$. The first and highest band is written in ascending "column form" starting from $\omega_{S1.L}$, and the second band is written in ascending "row form" starting from $\omega_{S2.L}$. Two band structures of this type are possible, but the one in which the column band is higher than the row band appears to give the simplest antialiasing constraints.[3] The corresponding DSB version of the identity wave is defined as

$$I_{\mathrm{DSB}}(t) = k_i \sum_{i=0}^{n-1} \cos\left(\omega_{IL_i} t\right) + \cos\left(\omega_{IU_i} t\right); \qquad k_i = \frac{1}{\sqrt{n}} \tag{13}$$

where $\boldsymbol{\omega_{\mathbf{IL}}}$ and $\boldsymbol{\omega_{\mathbf{IU}}}$ are identity frequency vectors that contain "diagonal frequencies" of the lower- and upper-sidebands of the attractor wave, respectively. These frequency bands are obtained by subtracting and adding, respectively, the *coding* bands in vector form

$$\boldsymbol{\omega_{\mathbf{IL}}} = \boldsymbol{\omega_{\mathbf{S1}}} - \boldsymbol{\omega_{\mathbf{S2}}}, \qquad \boldsymbol{\omega_{\mathbf{IU}}} = \boldsymbol{\omega_{\mathbf{S1}}} + \boldsymbol{\omega_{\mathbf{S2}}}. \tag{14}$$

The attractor wave, a spectral equivalent of (4), may be transmitted to a spectral neural decoder over a noisy channel. Encoded within the LSB of $W_{\mathrm{DSB}}(t)$ is a spectral attractor for each of the encocded patterns. In-phase coding generates an upper-sideband, diverting energy away from the LSB and complicating antialiasing constraints.[4] A 2-D illustration of autoassociative modulation is given in Fig. 4.

When more than one encoded pattern is superimposed in the same attractor wave, interference occurs and average signal power is pattern-dependent. However, for single patterns average signal power may be normalized by setting

$$k_w = \sqrt{\frac{P_s}{n-1}} \tag{15}$$

where P_s is the desired average signal power.

Although it is possible to recover the original patterns without filtering or canceling the USB, only half the available energy is used and satisfying the antialiasing constraints may require

[3]Interestingly, when the first band is higher than the second, generation of the memory wave is analogous to electrons jumping from higher to lower energies, emitting photons with "difference energy" into the electromagnetic field; i.e., into the LSB of the memory wave.

[4]In a complex formulation, the upper-sideband cancels out [29].

too much bandwidth. A SSB memory wave may be formed by *quadrature coding* as follows:

$$M_{\mathrm{SSB}}^{(m)}(t) = k_m \left(s_{I1}^{(m)}(t) s_{I2}^{(m)}(t) + s_{Q1}^{(m)}(t) s_{Q2}^{(m)}(t) \right) \qquad k_m = \sqrt{n} \tag{16}$$

where the quadrature waves are defined as

$$s_{Q1(2)}^{(m)}(t) = k_{s1(2)} \sum_{i=0}^{n-1} b_i^{(m)} \sin\left(\omega_{S1(2)i} t\right); \qquad k_{s1(2)} = \frac{1}{\sqrt{n}} \tag{17}$$

and $s_{I1(2)}(t)$ are the same as before. The SSB attractor wave may now be formed, where the SSB identity wave is

$$I_{\mathrm{SSB}}(t) = k_i \sum_{i=0}^{n-1} \cos\left(\omega_{IL_i} t\right); \qquad k_i = \frac{1}{\sqrt{n}}. \tag{18}$$

For single patterns ($p = 1$), signal power may be normalized by setting

$$k_w = \sqrt{\frac{2P_s}{n-1}}. \tag{19}$$

B. Spectral Recall

Spectral recall is realized by *recurrent associative demodulation* consisting of four parts: 1) initialization; 2) spectral synthesis; 3) spectral convolution; and 4) spectral analysis and update. Fig. 3(b) shows the decoder in block diagram form. The attractor wave, $W(t)$, is spectrally convolved with the *state wave*, $v(t)$, of the decoder, to produce the *virtual activation wave*, $a(t)$, in which linear activation information resides. This information is directly converted to dc, integrated, and quantized to update the neural states. Recalled data bits are simultaneously represented in the spatial domain as quantized neural states and in the frequency domain as *quantized phase of oscillation*. Local changes in phase are driven by the tendency of the Hopfield formalism to reduce global network energy over time, despite the presence of noise, and the neural state settles into *one* of the basins of attraction set up by the attractor wave. Regardless of formulation, i.e., in-phase or quadrature, autoassociative or heteroassociative, the physical architecture of the decoder is the same; only the frequencies that establish virtual connectivity are different.

1) Initialization: To minimize convergence time, linear activations u_i may be set to small values relative to the integration rate at the beginning of each decoding period. See Fig. 3(b). These values serve as initial conditions, the sign of which may be determined by the state of the decoder in the previous period, or may be the same each period. These values must not be set too far in either direction, since the more deeply the channels are driven into saturation, the longer it takes to pull them back out if necessary.

2) Spectral Synthesis: Spectral synthesis is the construction of the state wave, $v(t)$, which represents the state of the neural decoder in the frequency domain. The state wave is a sum of n synchronized cosine waves[5] given by

$$v(t) = \sum_{i=0}^{i-1} v_i \cos(\omega_{Vi} t) \tag{20}$$

where $v_i \in \{-1, +1\}$, with state synthesis frequencies ω_{Vi} defined in descending row form,[6] starting one $\Delta\omega$ away from the LSB of the attractor wave as follows:

$$\omega_{V_i} = \omega_{V.H} - i\Delta\omega \tag{21}$$

$\omega_{V.H}$ is the highest state frequency defined as

$$\omega_{V.H} = B_{S.GAP} + B_{S1} + 2B_{S2} + \Delta\omega \tag{22}$$

where $B_{S1} = n(n-1)\Delta\omega$ and $B_{S2} = (n-1)\Delta\omega$ are the respective coding bandwidths.

3) Spectral Convolution: Local changes in neural state are determined by linear combinations of extrinsic data from all over the network and the attractor wave, which would ordinarily require massive, nonlocal connectivity in spatial form. Fortunately, nonlocal connectivity may be achieved virtually in the frequency domain by spectral convolution, or temporal multiplication (mixing) as follows:

$$a(t) = W(t)v(t). \tag{23}$$

Spectral convolution, or associative demodulation, generates N linear combinations in the LSB of the activation wave $a(t)$ without having to directly connect every neuron to every other neuron! The same 2-D example from Fig. 4 is continued in Fig. 5 for the sake of illustrating associative demodulation.

4) Spectral Analysis and Update: Neural activation may be extracted from the activation wave by direct, local conversion followed by integration and the neural states are continuously quantized as follows:

$$v_i = \mathrm{sgn}(u_i); \qquad u_i = c \int a(t) \cos(\omega_{Ai} t)\, dt \tag{24}$$

where

- u_i linear state of the ith virtual neuron;
- v_i bipolar state of the ith virtual neuron;
- ω_{Ai} ith *analysis frequency*;
- c learning rate, which must be sufficiently small compared to the saturation limits on u_i.

Interestingly, and contrary to conventional wisdom, synchronous update can decrease BER when carried out at the same rate as asynchronous update, due to an increase in the number of state updates per iteration.

C. Antialiasing Constraints

Two antialiasing constraints must be satisfied to make autoassociative SAMs work. First, lower bounds are placed on frequency to prevent sideband aliasing and second, the "band gap" between coding bands must be wide enough such that the attractor wave is suitable for alias-free spectral convolution in

[5]Synchronized cosine waves are simultaneously *peaked*. Synchronized sine waves, on the other hand, are simultaneously *null*.

[6]Or alternatively in ascending column form, but the antialiasing constraints are stricter.

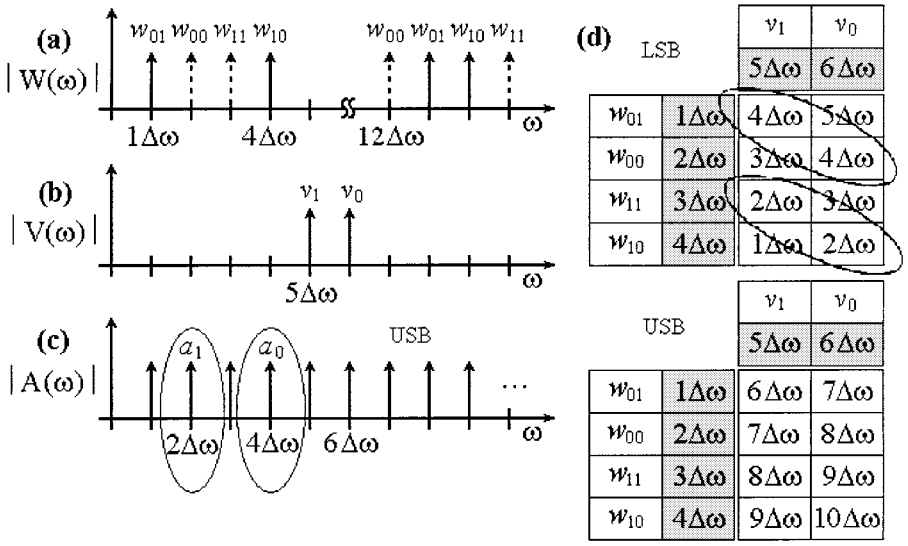

Fig. 5. Example of 2-D associative demodulation, continued from Fig. 4.

the decoder. The following formulation is designed for DSB attractor waves and therefore naturally works for SSB attractor waves as well.

Given the descending row form of the state band, the lower bound on the band gap, $B_{S.GAP}$ for preventing sideband aliasing in the activation wave is given as follows:

$$B_{S.GAP} > \frac{1}{2} B_{S2} \quad \Rightarrow \quad B_{S.GAP} = \text{ceil}\left(\frac{n}{2}\right) \Delta\omega \tag{25}$$

where $\text{ceil}(\cdot)$ rounds up to the next integer. Next, a lower bound is placed on $\omega_{S2.L}$ to prevent aliasing of the LSB of the activation wave by the USB of the attractor

$$\omega_{S2.L} > n^2 \Delta\omega \quad \Rightarrow \quad \omega_{S2.L} = (n^2 + 1)\,\Delta\omega \tag{26}$$

which also prevents aliasing in memory formation. This constraint is relaxed if the USB of the attractor is either filtered out or canceled by quadrature (or complex [29]) coding. The analysis vector may then be calculated by

$$\boldsymbol{\omega_A} = \boldsymbol{\omega_V} - \boldsymbol{\omega_{IL}}. \tag{27}$$

Consider a five-dimensional (5-D) example. The second coding band starts at $\omega_{S2.L} = 26\Delta\omega$ yielding $\boldsymbol{\omega_{S2}} = [26, 27, 28, 29, 30]^T\Delta\omega$. The band gap is calculated to be $B_{S.GAP} = 3\Delta\omega$, leading to $\boldsymbol{\omega_{S1}} = [33, 38, 43, 48, 53]^T\Delta\omega$. The identity frequency vectors are then $\boldsymbol{\omega_{IL}} = [7, 11, 15, 19, 23]^T\Delta\omega$ and $\boldsymbol{\omega_{IU}} = [59, 65, 71, 77, 83]^T\Delta\omega$, where $\boldsymbol{\omega_{IU}}$ is needed only for DSB attractors. Finally, the highest decoder state frequency is $\omega_{V.H} = B_{S.GAP} + (n^2 + n - 1)\Delta\omega = 32\Delta\omega$, leading to $\boldsymbol{\omega_V} = [32, 31, 30, 29, 28]^T\Delta\omega$ and $\boldsymbol{\omega_A} = [25, 20, 15, 10, 5]^T\Delta\omega$.

D. Scaling Complexity

Due to virtual nonlocal connectivity, spectral associative memories scale linearly with pattern dimension while maintaining high symbol-to-bit ratios. In addition to the two modulation mixers, gain blocks, and summers that are always present regardless of pattern dimension, autoassociative SAMs require $4n$ oscillators and mixers, split evenly between the encoder and decoder. These estimates assume large n where the identity wave shown in Fig. 3 has been omitted.

Multiplexing further reduces spatial complexity of the decoder. A multiplexed decoder requires $n + 1$ oscillators, one summer, two mixers, n quantizers and/or memory elements, and at least one filter. A multiplexed transconductance-mode (T-mode) circuit is depicted in Fig. 8 in which summation is realized in the current-domain.

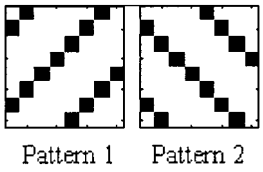

Fig. 6. Two 8 × 8 bit patterns used in dual-attractor simulation.

E. Dual-Attractor Example

A 64-bit (8 × 8) spectral network was simulated for the two binary images in Fig. 6. This size was chosen such that two memories could be reliably superposed and recalled without too much cross pattern interference. Two attractor waves were generated, one for each pattern, and simultaneously transmitted to the spectral neural decoder, each competing for attention. Depending partly on the initial conditions,[7] one of the two memories was recalled in every case, as shown in Fig. 7. In the first two trials, initial conditions were random and the network converged on one pattern or the other. In the third trial, initial conditions were biased toward pattern 2 and the network converged to pattern 2. In the last trial, initial conditions were biased toward the complement of pattern 1, and the network converged to the complement of pattern 1, as expected. The sample period (one iteration) was one microsecond and the bilinear transform[8] was

[7]Varying instantaneous power of attraction is a new characteristic of SAMs not present in the conventional formulation; i.e., a new way in which memory content may influence recall.

[8]The bilinear transform is one of several standard methods for mapping continuous time networks to discrete time.

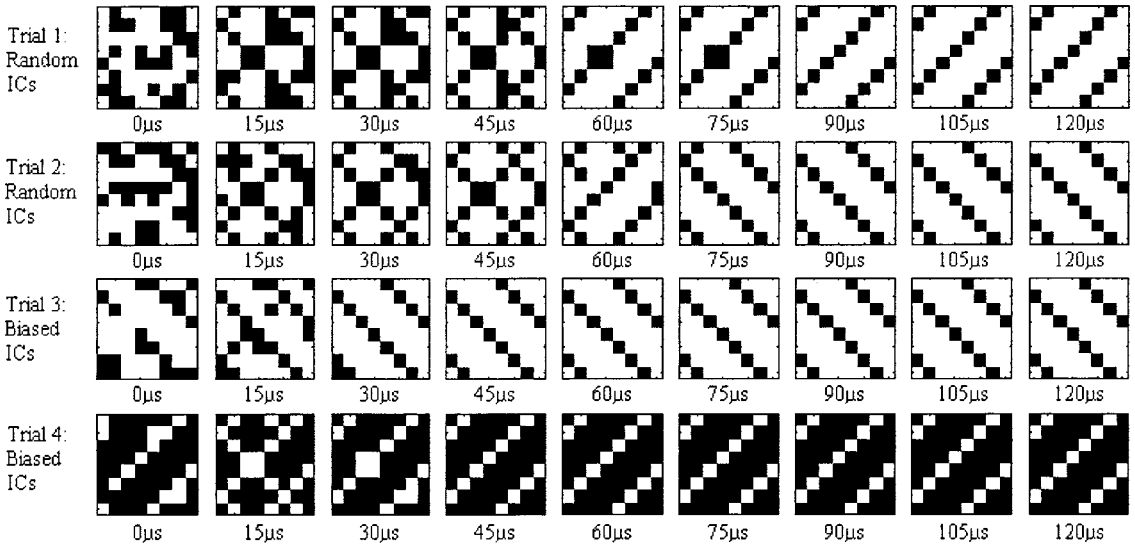

Fig. 7. Recall in the presence of dual attractors (two patterns; two spectral attractors).

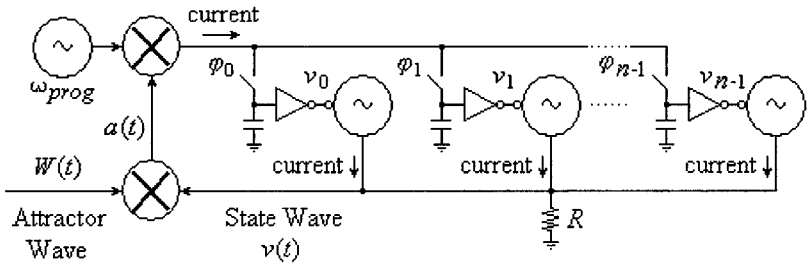

Fig. 8. Schematic of a current-mode multiplexed spectral decoder.

used to map the lossy integrators into the z-domain for updating the neural states. Low-pass poles were placed one decade below the carrier separation frequency of $\Delta f = 1$ kHz.

IV. Heteroassociative Spectral Memories

Multiple bit pattern *pairs* may be encoded and superimposed into heteroassociative attractor waves to form associations between two different patterns. Bit pattern pairs may be two images or alternatively, a *partitioning* of one larger image, as the case would be for simple communication applications. Although the autoassociative spectral memory may be shown to generalize the heteroassociative spectral memory when pattern pairs are made into one, subtle differences in band structure and antialiasing constraints exist when bandwidth must be conserved. The attractor wave is a direct linear superposition of the memory waves without diagonal cancellation

$$W(t) = k_w \sum_{m=1}^{p} M^{(m)}(t) \tag{28}$$

and recall follows in a similar manner to that of the autoassociative formulation where $n = \max(n_1, n_2)$. The scaling factors for in-phase heteroassociative coding are

$$k_{s1} = k_{s2} = \frac{1}{\sqrt{n}}, \qquad k_m = 2, \quad k_i = 0, \quad k_w = \sqrt{P_s} \tag{29}$$

and the scaling factors for quadrature heteroassociative coding are

$$k_{s1} = k_{s2} = \frac{1}{\sqrt{n}}, \qquad k_m = 1, \quad k_i = 0, \quad k_w = \sqrt{2P_s}. \tag{30}$$

A. Band Structures

Although they are typically at higher frequencies, heteroassociative coding bands may be *structured* the same as autoassociative coding bands. And the lowest frequency state band, corresponding to the second encoded bit pattern, may be structured in descending row form

$$\omega_{V2_i} = \omega_{V2.H} - i\Delta\omega. \tag{31}$$

The higher frequency state band, corresponding to the first encoded bit pattern, is given in ascending column form

$$\omega_{V1_i} = \omega_{V1.L} + ni\Delta\omega \tag{32}$$

where $i = 0, 1, \ldots n-1$ and $\omega_{V1.H}$ and $\omega_{V2.L}$, are the highest and lowest frequencies of the nonoverlapping first and second decoding state bands, respectively. Let the lowest band be one $\Delta\omega$ higher than the LSB of the attractor wave

$$\omega_{V2.H} = B_{S.GAP} + B_{S1} + 2B_{S2} + \Delta\omega \tag{33}$$

and let the higher state band be separated from the lower by a *decoding* band gap $B_{V.GAP}$

$$\omega_{V1.L} = \omega_{V2.H} + B_{V.GAP}. \tag{34}$$

Once the band structures have been defined, absolute frequencies may be calculated from antialiasing constraints.

B. Antialiasing Constraints

Although the band structures are similar to the autoassociative formulation, heteroassociative band structures must satisfy an additional antialiasing constraint to avoid *interlayer aliasing*, which causes the frequencies to be higher. Assuming the presence of an USB in the attractor wave, $B_{V.GAP}$ must be greater than either of the coding bandwidths

$$\begin{aligned} & B_{V.GAP} > \max(B_{S1}, B_{S2}) \\ \Rightarrow \quad & B_{V.GAP} = (n^2 - n + 1)\,\Delta\omega. \end{aligned} \tag{35}$$

When the first state band in descending row form is placed before the second band in ascending column form, $B_{S.GAP}$ is bounded by

$$\begin{aligned} & B_{S.GAP} > \tfrac{1}{2}(B_{S2} + B_{V.GAP}) \\ \Rightarrow \quad & B_{S.GAP} = \text{ceil}\left(\frac{n^2+1}{2}\right)\Delta\omega \end{aligned} \tag{36}$$

which is not as strict as that of the other permutation; i.e., if the second state band in ascending column form would have been placed before the first state band in descending row form. The second constraint, which prevents the USB of the attractor wave from aliasing the activation band is

$$\begin{aligned} & \omega_{S2.L} > \tfrac{3}{2}(B_{S1} + B_{S2}) + B_{V.GAP} + \Delta\omega \\ \Rightarrow \quad & \omega_{S2.L} = \text{ceil}\left(\tfrac{5}{2}n^2 - n + 1\right)\Delta\omega \end{aligned} \tag{37}$$

which is also not as strict as that of the other permutation. Absolute values may now be calculated for the analysis bands

$$\boldsymbol{\omega}_{\mathbf{A1(2)}} = \boldsymbol{\omega}_{\mathbf{V2(1)}} - \boldsymbol{\omega}_{\mathbf{IL}}. \tag{38}$$

Consider a 5-D example. Calculate the decoding band gap to be $B_{V.GAP} = B_{S1} + \Delta\omega = 21\Delta\omega$. The second coding band starts at $\omega_{S2.L} = 59\Delta\omega$, thus $\boldsymbol{\omega}_{\mathbf{S2}} = [59, 60, 61, 62, 63]^T\Delta\omega$. The coding band gap is calculated to be $B_{S.GAP} = 13\Delta\omega$, leading to $\boldsymbol{\omega}_{\mathbf{S1}} = [76, 81, 86, 91, 96]^T\Delta\omega$. The identity frequency vectors are then $\boldsymbol{\omega}_{\mathbf{IL}} = [17, 21, 25, 29, 33]^T\Delta\omega$ and $\boldsymbol{\omega}_{\mathbf{IU}} = [135, 141, 147, 153, 159]^T\Delta\omega$, where $\boldsymbol{\omega}_{\mathbf{IU}}$ is needed only for in-phase coding. Finally, the highest frequency in the lowest state band, corresponding to the first recalled bit of the second pattern, is $\omega_{V2.H} = 42\Delta\omega$. The lowest frequency in the highest state band, corresponding to the first recalled bit of the first pattern, is $\omega_{V1.L} = 63\Delta\omega$, leading to $\boldsymbol{\omega}_{\mathbf{V2}} = [42, 41, 40, 39, 38]^T\Delta\omega$, $\boldsymbol{\omega}_{\mathbf{V1}} = [63, 68, 73, 78, 83]^T\Delta\omega$, $\boldsymbol{\omega}_{\mathbf{A1}} = [25, 20, 15, 10, 5]^T\Delta\omega$, and $\boldsymbol{\omega}_{\mathbf{A2}} = [46, 47, 48, 49, 50]^T\Delta\omega$, where all elements are indexed in ascending order of recalled bits.

C. Scaling Complexity

The complexity of the heteroassociative encoder that partitions the same n-dimensional pattern as in the autoassociative formulation, is *half* that of the autoassociative encoder, but the decoder is the same. In addition to the two modulation mixers and summers that are always present regardless of pattern dimension, heteroassociative SAMs require n oscillators and mixers in the encoder and $2n$ oscillators and mixers in the decoder. The price for this reduction in complexity is lower noise immunity, and one additional decoding band and antialiasing constraint, which pushes the decoder bands higher.

V. Single-Attractor Networks for Digital Communications

Spectral associative memories lend themselves nicely to digital communications. Bit patterns, or *codewords*, may be transmitted as *transient spectral attractors*, one at a time, over a noisy channel to a spectral decoder. When only one attractor activates the decoder at a time, the initial conditions have no bearing on the steady state and one encoded bit pattern may be recovered with considerable noise immunity.

A. Complementary Attractor States

When only one codeword attractor is transmitted at a time, the virtual energy landscape contains *two* versions of the same systematic attractor: the codeword and its complement. As a result, one bit of overhead is required to distinguish between the two. Either the set of all possible codewords must be cut in half for a given codeword length, or the codeword must be increased by one *reference bit*. If the reference bit is always high and the corresponding bit in the decoder converges low, then all recalled data bits are inverted. One bit of overhead is sufficient for lower dimensional patterns, but as n increases, more than one ancillary bit may be needed.

B. Bit Error Rate

Spectral associative memories must tolerate *two* sources of noise: 1) initial condition noise and 2) attractor noise. In the conventional formulation, attractor noise is not significant and is typically ignored, but it is primarily this noise that SAMs must tolerate. In general, the received attractor wave, $W_{\text{noisy}}(t)$, may be a noisy version of the transmitted attractor wave as given by

$$W_{\text{noisy}}(t) = W(t) + \text{noise}(t) \tag{39}$$

where noise(t) may be modeled as white Gaussian noise. This noise is equivalent to "noisy weights" in the conventional formulation. Seven main factors influence BER:

1) carrier separation, or beat frequency Δf;
2) recall period T_c and pattern rate f_{s_pattern};
3) computational sampling rate f_{s_comp};
4) signal-to-noise ratio (SNR);
5) code rate R_c;
6) update method (synchronous or asynchronous);
7) initial conditions.

These factors are covered individually below.

1) Carrier Separation: The degree to which information is distributed over the frequency domain influences noise immunity. For a given n, spectrum spread is controlled by the carrier separation parameter, Δf (in Hz) or $\Delta\omega$ (in rad/s). The higher

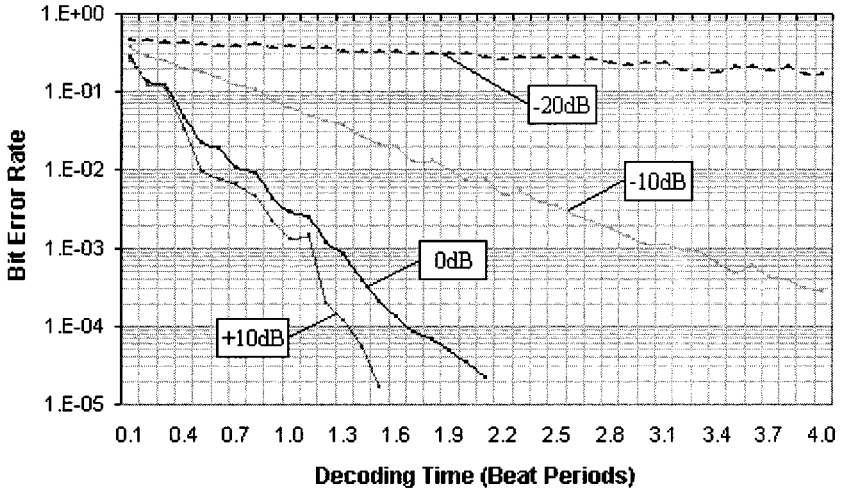

Fig. 9. BER versus decoding time for a five-bit (four data and one ancillary) autoassociative quadrature SAM for various SNRs with fixed carrier separation and computational sampling rate.

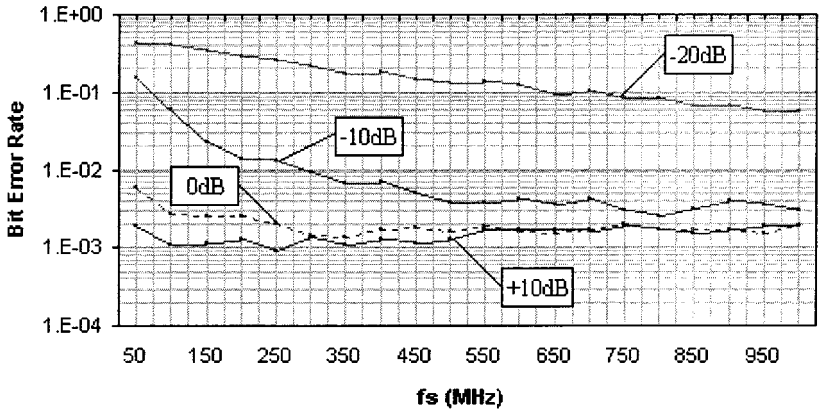

Fig. 10. BER versus computational sampling rate for a five-bit (four data bits and one overhead) autoassociative quadrature SAM for various SNRs with fixed carrier separation and decoding time.

Δf, the higher the noise immunity. The bandwidth of the LSB of the attractor wave is given by

$$B_W = B_{S1} + B_{S2} \tag{40}$$

for both autoassociative and heteroassociative cases, where B_{S1} and B_{S2} are the respective coding bands defined earlier.

2) Recall Period: Recall or convergence time, T_c, is also equal to the transmission period. The greater T_c, the lower the BER will be in the presence of white noise. Fortunately, white noise cannot move the decoder state anywhere over time because it provides no *colored motive*. Only the coherent part of the waveform instantiates the recall potential over time. T_c is generally limited by the beat period $1/\Delta f$ and the pattern sample period $T_{s\_\text{pattern}} = 1/f_{s\_\text{pattern}}$ as follows:

$$\frac{1}{\Delta f} \leq T_c \leq \frac{1}{f_{s\_\text{pattern}}} \tag{41}$$

where f_{s_pattern} is the pattern rate (number of n-bit patterns per second), which should be lower than the beat frequency. Ideally, T_c should be set equal to T_{s_pattern}, which should be an integer multiple of beats. Although the correct pattern may be recalled earlier, one beat period is the minimum time to achieve the desired average power P_s. Unlike conventional associative memories, instantaneous power of the attractor varies.

To demonstrate the effect of decoding time on SNR, a five-bit (four data bits and one ancillary bit) was simulated for random patterns, one at time, in the presence of additive white Gaussian noise. BER versus decoding time is shown in Fig. 9 for very noisy conditions in which four simulation sets were run for -20 dB, -10 dB, 0 dB, and 10 dB SNR; i.e., average signal power was 1/100, 1/10, 1, and 10 times the average noise power, respectively. As expected, BER always decreases with time, on the average. For example, for each additional beat in -10 dB SNR, BER decreased by approximately one decade. However, increasing SNR from 0 dB to 10 dB did not improve the BER as much as from -10 dB to 0 dB. The conditions of the simulations were as follows: one iteration was taken to be the equivalent of ten nanoseconds, the carrier separation parameter was $\Delta f = 100$ kHz, all blocks were ideal, and all oscillators were perfectly synchronized. Each point in the graph was obtained from enough simulations to observe at least 50 bit errors.

3) Computational Sampling Rate: When the encoder and decoder are implemented in discrete time, the *computational sample rate*, f_{s_comp}, must be much higher than the *data pattern rate*, f_{s_pattern}, to satisfy the Nyquist rate for coding and

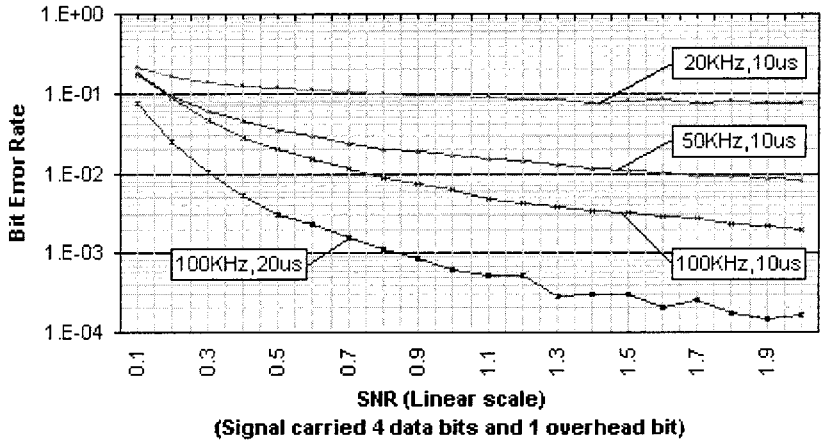

(a)

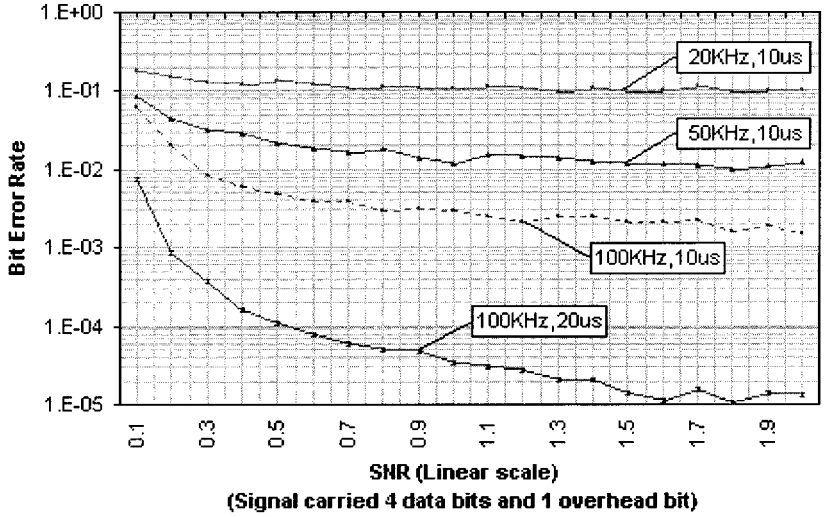

(b)

Fig. 11. BER versus SNR for different five-bit (four data and one ancillary) autoassociative SAMs for various decoding times and carrier separation, with fixed computational sampling rate: (a) in-phase (DSB) and (b) quadrature (SSB).

recall. Together, f_{s_comp} and f_{s_pattern} determine the number of iterations, or state updates, K per decoding period. For $T_c = T_{s\_\mathrm{pattern}}$, the number of iterations is determined by the ratio of sampling rates

$$K = \frac{T_c}{T_{s\_\mathrm{comp}}} = \frac{f_{s\_\mathrm{comp}}}{f_{s\_\mathrm{pattern}}}. \tag{42}$$

K should be much higher than one to avoid aliasing and decrease BER. The higher f_{s_comp}, the greater the number of state updates and the lower the error of recall will be, to a point.

Simulations were performed in which decoding time, carrier separation, and SNR were fixed and f_{s_comp} was varied. The results of these simulations are included in Fig. 10. These simulations show that the attractor wave carries a limited amount of information per unit time, as the Shannon limit would suggest. Since the decoding time was fixed, the transmitted energy from the decoder was also fixed, for a given SNR; thus the BER eventually flattened out as f_{s_comp} was increased. The bilinear transform was used to keep the effective learning rate constant regardless of f_{s_comp}. For instance, if the number of iterations per unit time was doubled, the integration gain was halved to keep the product constant. Thus, any change in the BER could be attributed to a change in f_{s_comp} and not to the effective learning rate.

4) Signal-to-Noise Ratio: To see the effect of noise, simulations were conducted on five-bit in-phase and quadrature SAMs for various degrees of SNR, carrier separation, and decoding time. The conditions of the simulations were as follows: one microsecond was taken to be the equivalent of 100 state updates, the decoder was perfectly synchronized with the encoder, and all computation was linear and high precision. The previous state was not retained from period to period and one ancillary bit was used to distinguish between complementary attractor states. Linear SNR was calculated and confirmed to be

$$\mathrm{SNR}_{\mathrm{linear}} = \frac{\frac{1}{K}\sum_{k=0}^{K-1}\left[W\left(kT_{s\_\mathrm{comp}}\right)\right]^2}{\frac{1}{K}\sum_{k=0}^{K-1}\left[\mathrm{noise}\left(kT_{s\_\mathrm{comp}}\right)\right]^2} = \frac{P_s}{\sigma^2} \tag{43}$$

where

T_{s_comp} set to 10 ns;
σ^2 noise power to be varied;
T_c decoding period, also to be varied.

Since the out-of-band noise was not filtered before recall, the decoder bandlimited the noise and signal at the same rate, making the power and energy ratios equal when taken over an integer multiple of beats. Wherever SNR was expressed in dB, it was calculated as 10 log($\text{SNR}_{\text{linear}}$) since power is calculated from the signal squared.

The results are shown in Fig. 11. In Fig. 11(a) the USB of the attractor wave was present, due to in-phase decoding, whereas in Fig. 11(b) it was not, due to quadrature coding. For $T_c \leq 1/\Delta f$, there was not much difference between the in-phase and quadrature formulations other than the inefficient use of the channel bandwidth in the former. However, when T_c was longer than one beat, there was a noticeable improvement in BER with quadrature coding.

5) Code Rate: Due to the nature of associative modulation, the code rate is determined by codeword *length* for both auto- and heteroassociative cases, and codeword *partitioning*, for the heteroassociative case only. Unlike other recursive schemes like turbo and low-density parity check coding, the amount of extrinsic redundancy is tightly coupled with the length of the codeword. Due to full virtual interconnectivity, autoassociative memories realize the highest noise immunity for n-bit codewords; i.e., a symbol-to-bit ratio of $n-1$

$$\left.\frac{E_s}{E_b}\right|_{\text{Autoassociative}} = \frac{n(n-1)}{n} = n-1. \tag{44}$$

For the same n bits, heteroassociative partitioning achieves more compact physical architectures at the expense of noise immunity. For an (n_1, n_2) partitioning of n bits, a ratio of $n_2:1$ is realized for first layer bits and a ratio of $n_1:1$ is realized for second layer bits

$$\left.\frac{E_s}{E_b}\right|_{\text{1st}-\text{HeteroLayer}} = \frac{n_1 n_2}{n_1} = n_2 \tag{45}$$

$$\left.\frac{E_s}{E_b}\right|_{\text{2nd}-\text{HeteroLayer}} = \frac{n_2 n_1}{n_2} = n_1. \tag{46}$$

Thus, the most significant bits of a digital word may be encoded with more redundancy than less significant bits.

An interesting feature of the heteroassociative decoder is that it is physically the same as the autoassociative decoder; i.e., only the frequencies differ. Thus, the virtual architecture, and therefore codeword partitioning and extrinsic redundancy, may be reprogrammed on the fly as noise conditions change.

6) Synchronous versus Asynchronous Update: The state of the spectral decoder may be updated either synchronously or asynchronously. Whereas conventional associative memories should be updated asynchronously to avoid limit cycles, SAMs appear to benefit from synchronous update and limit cycles do not seem to occur. Certainly BER is reduced by synchronous update for low computational sample rates.

7) Initial Conditions: In general, initial conditions may be fixed from decoding period to decoding period, but if successive codewords are samples of a continuous quantity, the decoder may be initialized with the previous state to reduce the hamming distance between initial and final states. However, the linear states must not be too large, since the more deeply the quantizers are driven into saturation, the longer it takes to pull them back out, if necessary.

VI. Conclusion

Spectral associative memories were proposed and characterized in the presence of noise for application in the field of communications. Due to the spectral representation of memories, network attractors exist in the frequency domain, separate from the neural decoder. Nonlocal neural connectivity is realized *virtually* in the frequency domain, allowing SAM networks to scale linearly with pattern dimension. Bit patterns may be enfolded into attractor waves creating extrinsic information and thus coding gain and noise immunity.

As in the conventional formulations, the possibility exists for content addressability; i.e., *multiple* patterns may be encoded and superposed into the same attractor wave, where each memory pattern competes for attention in the spectral decoder; however, cross-pattern interference and spurious attraction cause problems when patterns are small. For simple communication applications where the objective is to reliably send data over a noisy channel, one pattern may be transmitted at a time, each setting up a temporary basin of attraction in the decoder. The initial conditions are then irrelevant in terms of the steady state, and the content addressable feature is not exploited. Thus, rather than actually storing a set of exemplar waveforms in the decoder and computing the similarity of the received waveform with each exemplar by correlation, nothing is stored in the decoder and only one spectral attractor exists at a time. In this way, spurious attraction is eliminated.

Furthermore, extrinsic redundancy is a natural consequence of associative modulation, hence, SAMs have built-in noise immunity. While the autoassociative SAM achieves the highest noise immunity, the heteroassociative SAM offers the additional flexibility of achieving various code rates, or degrees of redundancy. The virtual architectures are nearly the same, with slight differences in band structure and antialiasing constraints.

In-phase and quadrature formulations were given for both associative forms, along with antialiasing constraints and examples. The performance of a five-bit autoassociative SAM was characterized in the presence of white Gaussian noise for various degrees of SNR, beat frequency, decoding time, and sampling rate. BER was shown to decrease with decoding time and in principle can be arbitrarily small in very noisy conditions given sufficient decoder sensitivity and synchronization, but is limited by the Shannon theorem as the sampling rate goes to infinity.

References

[1] J. Hopfield, "Neural networks and physical systems with emergent collective computational abilities," in *Proc. Nat. Academy Sci.*, vol. 79, 1982, pp. 2554–2558.
[2] Y. Abu-Mostafa and J. St. Jacques, "Information capacity of the Hopfield model," *IEEE Trans. Inform. Theory*, vol. IT-7, pp. 1–11, 1985.
[3] J. D. Keeler, "Basins of attraction of neural network models," in *Neural Networks for Computing*, J. S. Denker, Ed. College Park, MD: AIP, 1986, vol. 151.

[4] K. F. Cheung, L. E. Atlas, and R. J. Marks II, "Synchronous versus asynchronous behavior of Hopfield's content addressable memory," *Appl.Opt.*, vol. 26, pp. 4408–4813, 1987.
[5] T. Kohonen, *Content Addressable Memories*, 2nd ed. Berlin, Germany: Springer-Verlag, 1987.
[6] M. H. Hassoun, *Associative Neural Memories: Theory and Implementation*, M. H. Hassoun, Ed. Oxford, U.K.: Oxford Univ. Press, 1993.
[7] B. Kosko, "Adaptive bidirectional associative memories," *Appl. Opt.*, vol. 26, no. 23, pp. 4947–4959, 1987.
[8] ——, "Bidirectional associative memories," *IEEE Trans. Syst., Man, Cybern.*, vol. 18, pp. 49–60, 1988.
[9] G. X. Ritter, P. Sussner, and J. L. Diaz-de-Leon, "Morphological associative memories," *IEEE Trans. Neural Networks*, vol. 9, Mar. 1998.
[10] B. Linares-Barranco, E. Sanchez-Sinencio, A. Rodríguez-Vázquez, and J. L. Huertas, "A CMOS analog adaptive BAM with on-chip learning and weight refreshing," *IEEE Trans. Neural Networks*, vol. 4, pp. 445–455, May 1993.
[11] ——, "CMOS analog neural network systems based on oscillatory neurons," in *1992 IEEE Int. Symp. Circuits Syst.*, vol. 5, 1992, pp. 2236–2239.
[12] M. Verleysen and P. G. A. Jespers, "An analog VLSI implementation of Hopfield's neural network," *IEEE Micro.*, vol. 9, no. 6, pp. 46–55, Dec. 1989.
[13] R. L. K. Mandisodza, D. M. Luke, and P. Pochec, "VLSI implementation of a neural network classifier," in *1996 Canadian Conf. Elect. Comput. Eng.*, vol. 1, May 1996, pp. 178–181.
[14] A. Johannet, L. Personnaz, G. Dreyfus, J. D. Gascuel, and M. Weinfeld, "Specification and implementation of a digital Hopfield-type associative memory with on-chip training," *IEEE Trans. Neural Networks*, vol. 3 4, pp. 529–539, Jul. 1992.
[15] D. Psaltis and N. Farhat, "Optical information processing based on an associative-memory model of neural nets with thresholding and feedback," *Opt. Lett.*, vol. 10, p. 98, 1985.
[16] D. Psaltis, D. Brady, X. Gu, and S. Lin, "Holography in artificial neural networks," *Nature*, vol. 343, pp. 325–330, 1990.
[17] D. Gabor, "A new microscopic principle," *Nature*, vol. 161, p. 777, 1948.
[18] ——, "Associative holographic memories," *IBM J. Res. Dev.*, vol. 156, 1969.
[19] T. Poggio, "On holographic models of memory," *Kybernetik*, vol. 12, pp. 237–238, 1973.
[20] Y. Owechko, "Nonlinear holographic associative memories," *IEEE J. Quantum Electron.*, vol. 25, no. 3, Mar. 1989.
[21] D. Psaltis and F. Mok, "Holographic memories," *Sci. Amer.*, pp. 70–76, Nov. 1995.
[22] L. O. Chua and L. Yang, "Cellular neural networks: Theory," *IEEE Trans. Circuits Syst.*, vol. 35, pp. 1257–1272, Oct. 1988.
[23] L. O. Chua, T. Roska, and P. L. Venetianer, "The CNN is as universal as the Turing machine," *IEEE Trans. Circuits Syst.*, vol. 40, pp. 289–291, Apr. 1993.
[24] C. C. Lee and J. Pineda de Gyvez, "Color image processing in a cellular neural network environment," *IEEE Trans. Neural Networks*, vol. 7, pp. 1086–1098, Sept. 1996.
[25] R. Spencer, "Nonlinear spectral associative memories: Neural encoders and decoders for digital communications," in *Intelligent Engineering Systems Through Artificial Neural Networks*, C. H. Dagli, A. L. Buczac, J. Ghosh, M. J. Embrechts, O. Ersoy, and S. Kercel, Eds. New York: ASME Press, 2000, vol. 10, pp. 971–976.
[26] ——, "Nonlinear heteroassociative spectral memories: Virtually partitioned neural encoders and decoders for digital communications," in *2000 Int. Symp Comput. Intell. Int. Congr. Intell. Syst. Applicat.*, Wollongong, Australia, Dec. 12–15, 2000.
[27] D. Bohm and B. J. Hiley, *The Undivided Universe*: Routledge, Mar. 1995.
[28] A. Mondragon, R. Carvajal, J. Pineda de Gyvez, and E. Sanchez-Sinencio, "Frequency domain intrachip communication schemes for CNN," in *5th IEEE Int. Workshop. Cellular Neural Networks Their Applicat.*, London, U.K., Apr. 14–18, 1998.
[29] R. Spencer, "Single-pattern spectral associative memories for analog and digital communications," Int. J. Smart Eng. Syst. Design, 2001, to be published.

Ronald G. Spencer (S'97–M'99) received the B.S. degree in electrical engineering from the GMI Engineering and Management Institute, Kettering University, Flint, MI, in 1991, and the M.Sc. degree in bioengineering and Ph.D. degree in electrical engineering from Texas A&M University, College Station, in 1994 and 1999, respectively.

He was with General Motors Corporation from 1986 to 1991 as a Coop Student six months of every year, where he designed and implemented automatic bottleneck recognition systems in the main body build process of the Pontiac Grand Prix, Fairfax Plant, Kansas City, KS. In 1991, he continued as a Systems Engineer, writing and maintaining control software for automatic guided vehicles (AGVs) and programmable logic controllers (PLCs). From 1994 to 1996, he worked at OI Analytical and a Control Systems Programmer and in 1997 to 1998, interned at Oak Technology, where he designed printed circuit boards and Windows 95 software for audio CODEC testing and designed DVD read channel circuitry. He has been lecturing at Texas A&M since 1999 in the area of microelectronics and filters and conducting research on spectral neural networks for analog and digital communications and biometric sensors and processors for human face recognition and tracking. His long-term interests include spectral neural networks, quantum electronics, integrated antennas, and nanosensors.

Dr. Spencer was the recipient of the *2000 Artificial Neural Networks In Engineering* (ANNIE 200) Best Paper Award in "*Theoretical Developments in Computation Intelligence*."